Eidgenössische
Technische Hochschule
Zürich

Ecole polytechnique fédérale de Zurich
Politecnico federale di Zurigo
Swiss Federal Institute of Technology Zurich

Stable numerical scheme for the magnetic induction equation with Hall effect

P. Corti

Research Report No. 2010-30
October 2010

Seminar für Angewandte Mathematik
Eidgenössische Technische Hochschule
CH-8092 Zürich
Switzerland

Stable Numerical Scheme for the Magnetic Induction Equation with Hall Effect

Paolo Corti
Seminar for Applied Mathematics, ETH Zurich
CH-8092, Switzerland
E-mail: paolo.corti@sam.math.ethz.ch

Abstract

Fast magnetic reconnection can be modeled by Hall MHD equations. We consider a sub-model: the Hall induction equations and design stable finite difference schemes to approximate it. Numerical examples are provided to verify the robustness of the scheme.

1 Introduction

Magnetic reconnection, a widely studied phenomena in plasma physics, is a change of topology of the magnetic field lines that permits a fast change of the magnetic energy into thermal and kinetic energy. One of popular models for fast reconnection [1], are the equations of the form :

$$\frac{\partial \rho}{\partial t} = -\nabla \cdot (\rho \mathbf{u}) \tag{1.1}$$

$$\frac{\partial (\rho \mathbf{u})}{\partial t} = -\nabla \left\{ \rho \mathbf{u} \otimes \mathbf{u} + \left(p + \frac{|\mathbf{B}|^2}{2} \right) \mathbf{I}_{3\times 3} - \mathbf{B} \otimes \mathbf{B} \right\} \tag{1.2}$$

$$\frac{\partial \mathcal{E}}{\partial t} = -\nabla \left\{ \left(\mathcal{E} + p + \frac{|\mathbf{B}|^2}{2} \right) \mathbf{u} + \mathbf{E} \times \mathbf{B} \right\} \tag{1.3}$$

$$\frac{\partial \mathbf{B}}{\partial t} = -\nabla \times \mathbf{E}. \tag{1.4}$$

Here ρ, $\mathbf{u}$, p are the gas density, velocity and pressure respectively. $\mathbf{E}$ and $\mathbf{B}$ are the electric and magnetic fields. The total energy $\mathcal{E}$ is given by the equation of state, i.e.,

$$\mathcal{E} = \frac{p}{\gamma - 1} + \frac{\rho |\mathbf{u}|^2}{2} + \frac{|\mathbf{B}|^2}{2}. \tag{1.5}$$

Here γ is the gas constant. Equations from (1.1) to (1.3) represent the conservation of mass, momentum and energy; the last one (1.4) describes

the evolution of the magnetic field.
The equations have to obey the divergence constraint:

$$\nabla \cdot \mathbf{B} = 0. \tag{1.6}$$

For ideal MHD, the electric field is given by

$$\mathbf{E} = -\mathbf{u} \times \mathbf{B}. \tag{1.7}$$

However, no reconnection is possible with this model. In order to model fast reconnection, we use a generalized Ohm's law [2],[3]

$$\mathbf{E} = -\mathbf{u} \times \mathbf{B} + \eta \mathbf{J} + \frac{\delta_i}{L_0} \frac{\mathbf{J} \times \mathbf{B}}{\rho} + \left(\frac{\delta_e}{L_0}\right)^2 \frac{1}{\rho} \left[\frac{\partial \mathbf{J}}{\partial t} + (\mathbf{u} \cdot \nabla) \mathbf{J}\right]. \tag{1.8}$$

Here L_0 is the normalizing length unit, and δ_e and δ_i denote electron and ion inertia respectively; they are related to electron-ion mass ratio by $(\frac{\delta_e}{\delta_i})^2 = \frac{m_e}{m_i}$.
Using the Ampère's law we can write the electric current $\mathbf{J}$ as

$$\mathbf{J} = \nabla \times \mathbf{B}. \tag{1.9}$$

The Hall MHD equations are non-linear and complicated. A sub-model is the Hall induction equation given by

$$\begin{aligned} \frac{\partial}{\partial t}\left[\mathbf{B} + \left(\frac{\delta_e}{L_0}\right)^2 \nabla \times (\nabla \times \mathbf{B})\right] &= \nabla \times (\mathbf{u} \times \mathbf{B}) - \eta \nabla \times (\nabla \times \mathbf{B}) \\ &- \left(\frac{\delta_e}{L_0}\right)^2 \frac{1}{\rho} \nabla \times ((\mathbf{u} \cdot \nabla)(\nabla \times \mathbf{B})) - \frac{\delta_i}{L_0} \frac{1}{\rho} \nabla \times ((\nabla \times \mathbf{B}) \times \mathbf{B}) \end{aligned} \tag{1.10}$$

with $\mathbf{u}$ being a given velocity field.
For the remaining part of this paper, we will focus on the Hall induction equations (1.10) and onto the design stable numerical scheme for it.

2 Theoretical Analysis

We rewrite the advection term in (1.10) using a standard vector identity resulting in

$$\nabla \times (\mathbf{u} \times \mathbf{B}) = (\mathbf{B} \cdot \nabla)\mathbf{u} - \mathbf{B}(\nabla \cdot \mathbf{u}) + \mathbf{u}(\nabla \cdot \mathbf{B}) - (\mathbf{u} \cdot \nabla)\mathbf{B} \tag{2.1}$$

We note that the term that leads to a lack of symmetry is $\mathbf{u}(\nabla \cdot \mathbf{B})$. For divergence free data (1.6) this term vanishes and the remaining equations are in symmetric form:

$$\frac{\partial}{\partial t}\left[\mathbf{B}+\left(\frac{\delta_e}{L_0}\right)^2 \nabla\times(\nabla\times\mathbf{B})\right] = (\mathbf{B}\cdot\nabla)\mathbf{u}-\mathbf{B}(\nabla\cdot\mathbf{u})-(\mathbf{u}\cdot\nabla)\mathbf{B}$$
$$-\eta\nabla\times(\nabla\times\mathbf{B})-\left(\frac{\delta_e}{L_0}\right)^2\frac{1}{\rho}\nabla\times((\mathbf{u}\cdot\nabla)(\nabla\times\mathbf{B}))$$
$$-\frac{\delta_i}{L_0}\frac{1}{\rho}\nabla\times((\nabla\times\mathbf{B})\times\mathbf{B}) \tag{2.2}$$

We have the following theorem:

Theorem 2.1. *Let* $\mathbf{u}\in C^2(\mathbb{R}^3)$ *decays to zero sufficiently fast. Furthermore, assume that the solution of (2.2) goes to zero at infinity, then following apriori estimates hold:*

$$\frac{d}{dt}\left(\|\mathbf{B}\|^2_{L^2(\mathbb{R}^3)}+\left(\frac{\delta_e}{L_0}\right)^2\frac{1}{\rho}\|\nabla\times\mathbf{B}\|^2_{L^2(\mathbb{R}^3)}\right)$$
$$\leq C_1\left(\|\mathbf{B}\|^2_{L^2(\mathbb{R}^3)}+\left(\frac{\delta_e}{L_0}\right)^2\frac{1}{\rho}\|\nabla\times\mathbf{B}\|^2_{L^2(\mathbb{R}^3)}\right) \tag{2.3}$$

$$\frac{d}{dt}\|\nabla\cdot\mathbf{B}\|_{L^2(\mathbb{R}^3)}\leq C_2\|\nabla\cdot\mathbf{B}\|_{L^2(\mathbb{R}^3)} \tag{2.4}$$

with C_1 *and* C_2 *being constants that depend on* $\mathbf{u}$ *and its derivatives only. The above estimates imply that* $\mathbf{B}\in H^1_{loc}(\mathbb{R}^3)$.

Proof. For the first inequality we multiply the equation with $\mathbf{B}$ and then integrate over $\mathbb{R}^3$ resulting in

$$\int_{\mathbb{R}^3}\frac{1}{2}\frac{\partial\mathbf{B}^2}{\partial t}+\left(\frac{\delta_e}{L_0}\right)^2\frac{1}{\rho}\mathbf{B}\nabla\times(\nabla\times\frac{\partial\mathbf{B}}{\partial t})dx=$$
$$\int_{\mathbb{R}^3}\left[\mathbf{B}(\mathbf{B}\cdot\nabla)\mathbf{u}-\mathbf{B}^2(\nabla\cdot\mathbf{u})-\frac{1}{2}(\mathbf{u}\cdot\nabla)\mathbf{B}^2-\eta\mathbf{B}\nabla\times(\nabla\times\mathbf{B})\right.$$
$$\left.-\left(\frac{\delta_e}{L_0}\right)^2\frac{1}{\rho}\mathbf{B}\nabla\times((\mathbf{u}\cdot\nabla)(\nabla\times\mathbf{B}))-\frac{\delta_i}{L_0}\frac{1}{\rho}\mathbf{B}\nabla\times((\nabla\times\mathbf{B})\times\mathbf{B})\right]dx.$$

Partial integration yields

$$\frac{1}{2}\frac{d}{dt}\left(\|\mathbf{B}\|^2_{L^2(\mathbb{R}^3)}+\left(\frac{\delta_e}{L_0}\right)^2\|\nabla\times\mathbf{B}\|^2_{L^2(\mathbb{R}^3)}\right)=$$
$$\int_{\mathbb{R}^3}\left[\mathbf{B}(\mathbf{B}\cdot\nabla)\mathbf{u}-\frac{1}{2}\mathbf{B}^2(\nabla\cdot\mathbf{u})-\eta(\nabla\times\mathbf{B})^2\right.$$
$$\left.+\frac{1}{2}\left(\frac{\delta_e}{L_0}\right)^2\frac{1}{\rho}(\nabla\cdot\mathbf{u})(\nabla\times\mathbf{B})^2-\frac{\delta_i}{L_0}\frac{1}{\rho}\underbrace{(\nabla\times\mathbf{B})((\nabla\times\mathbf{B})\times\mathbf{B})}_{=0}\right]dx$$

Using the smoothness of u in the above identity leads to

$$\frac{d}{dt}\left(\|\mathbf{B}\|^2_{L^2(\mathbb{R}^3)} + \left(\frac{\delta_e}{L_0}\right)^2 \|\nabla\times\mathbf{B}\|^2_{L^2(\mathbb{R}^3)}\right) \leq$$
$$C_A\|\mathbf{B}\|^2_{L^2(\mathbb{R}^3)} + C_B\left(\frac{\delta_e}{L_0}\right)^2 \|\nabla\times\mathbf{B}\|^2_{L^2(\mathbb{R}^3)}$$

here $C_A = \max\limits_{k=\{x,y,z\}}(\|\frac{\partial(u_1+u_2+u_3)}{\partial k}\|_{L^\infty(\mathbb{R}^3)})$ and $C_B = \|\nabla\mathbf{u}\|_{L^\infty(\mathbb{R}^3)}$. Applying divergence operator on (2.2), we obtain

$$\frac{\partial\nabla\cdot\mathbf{B}}{\partial t} = -\nabla(\mathbf{u}(\nabla\cdot\mathbf{B})).$$

Integrating over $\mathbb{R}^3$ and then integration by parts, we obtain the estimate (2.4) by setting $C_2 = \|\nabla\mathbf{u}\|_{L^\infty(V)}$. □

3 Numerical Scheme

We subdivide the computational domain using a uniform Cartesian mesh with mesh width Δx,Δy and Δz. $\hat{\mathbf{B}}_{i,j,k}(t)$ and $\hat{\mathbf{u}}_{i,j,k}(t)$ are approximations of $\mathbf{B}(\mathbf{x},t)$ and $\mathbf{u}(\mathbf{x},t)$ at point (x_i,y_j,z_k). We also define discrete derivatives $\mathbf{D} = (D_x,D_y,D_z)^\top$ using central differences:

$$\begin{pmatrix} D_x \\ D_y \\ D_z \end{pmatrix} a_{i,j,k} = \begin{pmatrix} \frac{a_{i+1,j,k}-a_{i-1,j,k}}{2\Delta x}. \\ \frac{a_{i,j+1,k}-a_{i,j-1,k}}{2\Delta y}. \\ \frac{a_{i,j,k+1}-a_{i,j,k-1}}{2\Delta z}. \end{pmatrix} \tag{3.1}$$

where $a_{i,j,k}$ is an arbitrary function defined on the mesh. For central difference operators we have the following lemmas:

Lemma 3.1 (Summation by parts). *Let $a_{i,j,k}$ and $b_{i,j,k}$ be grid functions, such that $|a_{i,j,k}|,|b_{i,j,k}| \to 0$ for $i,j,k\to\infty$ then*

$$\sum_{i,j,k} a_{i,j,k}D_x b_{i,j,k} = -\sum_{i,j,k} b_{i,j,k}D_x a_{i,j,k} \tag{3.2}$$

Proof. This follow directly by a change of index in the sum. □

Lemma 3.2 (Discrete chain rule). *For every finite difference operator D that approximates the first derivative, there exists an averaging operator A such that for every $a_{i,j,k} = a(x_i,y_j,z_k)$ with $a\in C^2$ and every $b_{i,j,k}$ defined on the mesh,*

$$D(a_{i,j,k}b_{i,j,k}) = a_{i,j,k}D(b_{i,j,k}) + A(b_{i,j,k})D(a_{i,j,k}) + \tilde{a}_{i,j,k} \tag{3.3}$$

holds. If $b_{i,j,k}\in l^2$, then the residual $\tilde{a}$ is bounded i.e., $\|\tilde{a}\|\leq Ch\|b\|$ for a generic mesh size h and some constant $C>0$.

Proof. For the proof of this lemma, see [4] lemma 3.3. □

For approximating (2.2) we use the following semi-discrete numerical scheme

$$\frac{\partial}{\partial t}\left[\hat{\mathbf{B}}_{i,j,k} + \left(\frac{\delta_e}{L_0}\right)^2 \mathbf{D}\times(\mathbf{D}\times\hat{\mathbf{B}}_{i,j,k})\right] = \bar{\mathbf{A}}\left(\hat{\mathbf{B}}_{i,j,k}\cdot\mathbf{D}\right)\hat{\mathbf{u}}_{i,j,k}$$
$$-\mathbf{A}\left(\hat{\mathbf{B}}_{i,j,k}(\mathbf{D}\cdot\hat{\mathbf{u}}_{i,j,k})\right) - (\hat{\mathbf{u}}_{i,j,k}\cdot\mathbf{D})\hat{\mathbf{B}}_{i,j,k} - \eta\mathbf{D}\times(\mathbf{D}\times\hat{\mathbf{B}}_{i,j,k})$$
$$-\left(\frac{\delta_e}{L_0}\right)^2\frac{1}{\rho}\mathbf{D}\times((\hat{\mathbf{u}}_{i,j,k}\cdot\mathbf{D})\hat{\mathbf{B}}_{i,j,k}) - \frac{\delta_i}{L_0}\frac{1}{\rho}\mathbf{D}\times\left((\mathbf{D}\times\hat{\mathbf{B}}_{i,j,k})\times\hat{\mathbf{B}}_{i,j,k}\right). \tag{3.4}$$

Note that t is suppressed for notational convenience. We denote

$$\bar{\mathbf{A}}(\mathbf{B}_{i,j,k}\cdot\mathbf{D}) = A_x(B^1_{i,j,k})D_x + A_y(B^2_{i,j,k})D_y + A_z(B^3_{i,j,k})D_z \tag{3.5}$$

and

$$\mathbf{A}\left(\mathbf{B}_{i,j,k}(\mathbf{D}\cdot\mathbf{u}_{i,j,k})\right)^i =$$
$$A_x(B^i_{i,j,k})D_x u^1_{i,j,k} + A_y(B^i_{i,j,k})D_y u^2_{i,j,k} + A_z(B^i_{i,j,k})D_z u^3_{i,j,k} \tag{3.6}$$

for $i = 1, 2, 3$. A being the averaging operator defined in previous lemma. We can show that the following holds:

Theorem 3.3. *Let $\hat{\mathbf{u}}_{i,j,k} = \mathbf{u}(x_i, y_j, z_k)$ be the point evaluation of a function $u \in C^2$ and let the solutions of (3.4) go to zero at infinity, then the following estimates hold*

$$\frac{d}{dt}\left(\|\hat{\mathbf{B}}\|^2_{l^2(\mathbb{R}^3)} + \left(\frac{\delta_e}{L_0}\right)^2\frac{1}{\rho}\|\mathbf{D}\times\hat{\mathbf{B}}\|^2_{l^2(\mathbb{R}^3)}\right)$$
$$\leq C_1\left(\|\hat{\mathbf{B}}\|^2_{l^2(\mathbb{R}^3)} + \left(\frac{\delta_e}{L_0}\right)^2\frac{1}{\rho}\|\mathbf{D}\times\hat{\mathbf{B}}\|^2_{l^2(\mathbb{R}^3)}\right) \tag{3.7}$$

$$\frac{d}{dt}\|\mathbf{D}\cdot\hat{\mathbf{B}}\|^2_{l^2(\mathbb{R}^3)} \leq C_2\|\mathbf{D}\cdot\hat{\mathbf{B}}\|^2_{l^2(\mathbb{R}^3)} + C_3\max(\Delta x, \Delta y, \Delta z) \tag{3.8}$$

with C_1, C_2 and C_3 constant that depend on $\mathbf{u}$ *and its derivative only.*

Proof. The proof of this theorem uses the two lemmas 3.1 and 3.2 to mimic the proof of the continuous version of this theorem (Thm. 2.1). A detailed proof will be provided in [5]. □

The scheme (3.4) is semi-discrete and needs to be coupled with a suitable numerical time-integration routine. We have chosen to use a second-order SSP Runge-Kutta method [6].

Remark 3.4. A fourth order version of this scheme is derived by replacing the central difference operator by corresponding fourth-order central difference, e.g.,

$$D_x^{(4)} a_{i,j,k} = \frac{2}{3}\frac{a_{i+1,j,k} - a_{i-1,j,k}}{\Delta x} - \frac{1}{12}\frac{a_{i+2,j,k} - a_{i-2,j,k}}{\Delta x} \tag{3.9}$$

4 Numerical Experiments

We tested the numerical scheme for a 2-d version of the general induction equations(2.2) with the following initial data

$$\mathbf{B}_0(x,y) = 4\begin{pmatrix} -y \\ x-\frac{1}{2} \\ 0 \end{pmatrix} e^{-20((x-\frac{1}{2})^2+y^2)} \tag{4.1}$$

and $\mathbf{u} = (-y, x, 0)^\top$. An exact solution of this problem can be calculated in the pure advection case, i.e. if $\eta = \delta_i = \delta_e = 0$. The solution is given by

$$\mathbf{B}(x,y,t) = \mathbf{R}(t)\mathbf{B}_0(\mathbf{R}(-t)(x,y)) \tag{4.2}$$

where $\mathbf{R}(t)$ is a rotation matrix on the z axis with angular velocity t. We ran two different tests on the domain $[-2.5, 2.5] \times [-2.5, 2.5]$ with Dirichlet boundary conditions.

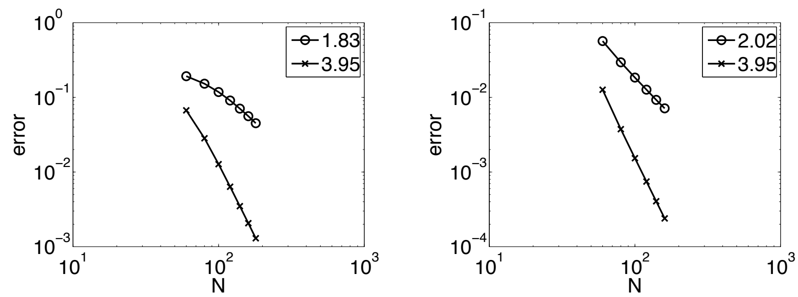

Figure 4.1: l^2 convergence analysis. On the left we have $\eta = \delta_i = \delta_e = 0$, and on the right the forced problem for $L_0 = \rho = 1$, $\eta = 0.01$,$\delta_i = 0.1$ and $\delta_e = 4.5 \times 10^{-2}$. In the legend we show the slope of the lines

Test 1 We test convergence of the scheme for two different central difference operators. One of second order and other of order four.
In absence of a known analytical solution in presence of Hall effect, we have modified the problem. We add known analytical source

term to the induction equation; this term is computed so that (4.2) is the solution of the forced version of (2.2).
In Fig. 4.1 we show l^2 errors after a time $t = 2\pi$ for different mesh size $N = N_x = N_y$. The theoretical orders of convergence are obtained.

Test 2 As second test we compare the solutions for advection problem and full problem at time $t = \pi$ (Fig.4.2). We note that that the resistivity and the Hall term diffuse the solution and also induce a creation of a small third component in the field.

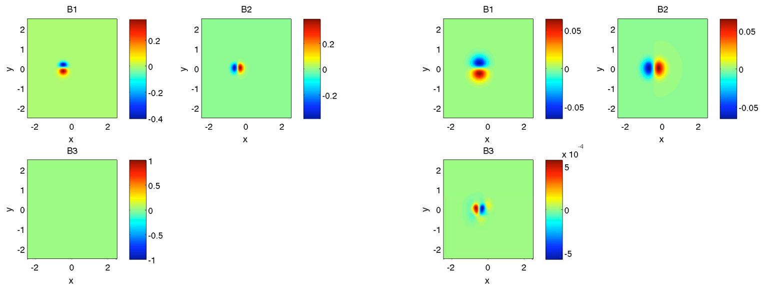

Figure 4.2: Solution after $T = \pi$. On the left we have $\eta = \delta_i = \delta_e = 0$, and on the right we have $L_0 = \rho = 1$, $\eta = 0.01$,$\delta_i = 0.1$ and $\delta_e = 4.5 \times 10^{-2}$.

5 Conclusion

The symmetric form of the general induction equations (2.2) posses some energy and divergence estimates. These estimates can be used to build a stable numerical scheme.
The presence of a time-derivative of the current in (2.2) implies that a matrix inversion has to be performed at every time step. Currently, we use a direct solver to invert the matrix. However, the matrix is ill conditioned and suitable pre-conditioners need to be devised to stabilize and accelerate the inversion algorithms. The design of such pre-conditioner is a topic of ongoing research and they will be presented in forthcoming papers.

References

[1] X.H.Deng and H. Matsumoto, Rapid magnetic reconnection in the Earth's magnetosphere mediated by whistler waves,(2001), Nature

410, 557-560.

[2] Z.W. Ma and A. Bhattacharjee, Hall magnetohydrodynamic reconnection: The Geospace Environment Modeling challenge, J.Geophys. Res, (2001), Vol 106, No. A3, 3773-3782.

[3] X. Qian, J. Balbás, A. Bhattacharjee and H. Yang, A Numerical Study of Magnetic Reconnection: A Central Scheme for Hall MHD, "Hyperbolic Partial Differential Equations, Theory, Numerics and Applications", Proceedings of the 12th international conference held at the University of Maryland, To appear.

[4] S. Mishra and M.Svärd, On stability of numerical schemes via frozen coefficient and the magnetic induction equations, BIT Numerical Mathematics, (2010), Vol. 50, pp. 85-108

[5] P.Corti and S. Mishra, Stable Finite Difference Scheme for the Magnetic Induction Equation with Hall Effect, in preparation

[6] S. Gottleib,C.W. Shu and E. Tadmor, High order time discretisation with strong stability property, SIAM Review,(2001),Vol 43, pp. 89-112

Research Reports

No.	Authors/Title
10-30	*P. Corti* Stable numerical scheme for the magnetic induction equation with Hall effect
10-29	*H. Kumar* Finite volume methods for the two-fluid MHD equations
10-28	*S. Kurz and H. Heumann* Transmission conditions in pre-metric electrodynamics
10-27	*F.G. Fuchs, A.D. McMurry, S. Mishra and K. Waagan* Well-balanced high resolution finite volume schemes for the simulation of wave propagation in three-dimensional non-isothermal stratified magneto-atmospheres
10-26	*U.S. Fjordholm, S. Mishra and E. Tadmor* Well-balanced, energy stable schemes for the shallow water equations with varying topography
10-25	*U.S. Fjordholm and S. Mishra* Accurate numerical discretizations of non-conservative hyperbolic systems
10-24	*S. Mishra and Ch. Schwab* Sparse tensor multi-level Monte Carlo finite volume methods for hyperbolic conservation laws with random intitial data
10-23	*J. Li, J. Xie and J. Zou* An adaptive finite element method for distributed heat flux reconstruction
10-22	*D. Kressner* Bivariate matrix functions
10-21	*C. Jerez-Hanckes and J.-C. Nédélec* Variational forms for the inverses of integral logarithmic operators over an interval
10-20	*R. Andreev* Space-time wavelet FEM for parabolic equations
10-19	*V.H. Hoang and C. Schwab* Regularity and generalized polynomial chaos approximation of parametric and random 2nd order hyperbolic partial differential equations
10-18	*A. Barth, C. Schwab and N. Zollinger* Multi-Level Monte Carlo Finite Element method for elliptic PDE's with stochastic coefficients